Generalized Sequential Model Predictive Control of IM Drives With Field-Weakening Ability

Yongchang Zhang, *Senior Member, IEEE*, Boyue Zhang, Haitao Yang, *Student Member, IEEE*, Margarita Norambuena, *Member, IEEE*, and Jose Rodriguez, *Fellow, IEEE*

***Abstract*—A very simple sequential model predictive control (SMPC) is recently proposed to achieve high performance control of induction motor drives. By evaluating two separate cost functions for the torque and amplitude of the stator flux linkage in a cascaded way, the weighting factor in the conventional MPC is eliminated. However, it is shown in this paper that the conventional SMPC cannot achieve stable operation over the full speed range, if the cost function for the stator flux linkage is first evaluated. To solve this problem, this paper proposes a generalized SMPC (GSMPC), which is effective when any one of the two cost functions is first evaluated. Compared to the conventional SMPC, GSMPC not only eliminates the limitation on the execution order of two cost functions, but also presents less stator flux ripples and lower current total harmonic distortion with even lower average switching frequency. Furthermore, a simple field-weakening strategy is proposed and combined with GSMPC to widen the speed range by adjusting the torque and stator flux linkage reference online. Both simulation and experimental results are presented to confirm the effectiveness of the proposed method.**

***Index Terms*—Field-weakening (FW) operation, induction motor (IM) drives, predictive control, torque control.**

I. Introduction

MODEL predictive control (MPC) has received wide attention in the control of ac motor drives owing to its merits of simple principle, quick response, and ability to handle multiple variables and nonlinear constraints [1], [2]. MPC selects the optimal voltage vector by evaluating a cost function, which is usually a combination of torque and flux linkage errors

Manuscript received August 18, 2018; revised October 26, 2018; accepted December 5, 2018. Date of publication December 11, 2018; date of current version June 10, 2019. This work was supported in part by the National Natural Science Foundation of China under Grant 51577003, in part by the Beijing Natural Science Foundation under Grant 3162012, in part by CONICYT under Grant Basal Project FB0008: Advanced Center for Electrical and Electronic Engineering (AC3E) and in part by FONDECYT under Grants 1170167 and 11180233. Recommended for publication by Associate Editor R. Kennel. *(Corresponding author: Haitao Yang.)*

Y. Zhang and B. Zhang are with the Inverter Technologies Engineering Research Center of Beijing, North China University of Technology, Beijing 100144, China (e-mail:

method evaluates the cost function for torque first and selects two vectors that have a smaller torque error than other candidate vectors. The two vectors are then sent to the second cost function to select the best one minimizing the flux linkage error. This cascaded structure is very simple and eliminates the use of the weighting factor. However, it is not analyzed how many candidate vectors should be selected from the first cost function. As there are only two vectors for the cost function of the stator flux linkage to evaluate, the conventional SMPC implies higher priority to the torque. If the cost function of the stator flux linkage amplitude is first evaluated and only two candidate vectors are selected for the second cost function of the torque, the drive system may fail to work and even lose its stability, as confirmed in this paper. Furthermore, if the control variables have equal importance, such as the stator current vector, stator flux linkage vector, or stator voltage vector, it is evidently inappropriate to assign more priority to the variable in the first cost function.

So far, field-weakening (FW) operation has not been fully considered in the MPC drives. In fact, FW operation is of great practical value, especially in the traction drives requiring high speed operation and electric vehicle drives with limited battery resource [14]. When induction motors (IMs) operate in a high-speed region, the goal is to produce the maximum torque and to fully exploit the machine and converter capabilities. The traditional method is to make the reference of the stator flux linkage inversely proportional to the motor speed when the rotor speed is above the rated speed [15]–[17]. However, it is not explicitly investigated whether the theoretical maximum load angle of 45° [18] has been reached except [16].

This paper proposes a generalized SMPC (GSMPC) strategy for IM drives to achieve a high performance control. The main contribution of this paper consists of the following two aspects. First, an improved GSMPC is proposed by slight modification of the prior SMPC. Similar to the conventional SMPC, the proposed GSMPC also uses a cascaded structure of torque control and flux linkage control, which selects the best voltage vector by sequentially evaluating two individual cost functions. However, different from the conventional SMPC, any one of the two cost functions can be evaluated first without limitation on the execution order. This not only improves the universality of the conventional SMPC, but also presents better steady-state performance with even lower switching frequency. Second, a simple but effective FW scheme is proposed and combined with the proposed GSMPC to significantly widen the speed range. The existing MPC schemes rarely investigate FW operation with maximum torque ability. In this paper, the optimal FW operation with maximum load limitation is studied by properly designing the maximum value of torque reference. The proposed GSMPC is compared to the conventional SMPC and its effectiveness is validated by the simulation and experimental results from a 2.2-kW IM drive system.

II. Model of IM

Taking stator flux linkage vector $\boldsymbol{\psi}_s$ and stator current vector $\boldsymbol{i}_s$ as state variables, the mathematical model of the IM in the stationary reference frame can be expressed as

$$\frac{\mathrm{d}\boldsymbol{x}}{\mathrm{d}t} = \boldsymbol{A}\boldsymbol{x} + \boldsymbol{B}\boldsymbol{u_s} \tag{1}$$

where $\boldsymbol{x} = [\,\boldsymbol{i}_s\ \boldsymbol{\psi}_s\,]^T$ are state variables, $\boldsymbol{u_s}$ is the stator voltage vector, and

$$\boldsymbol{A} = \begin{bmatrix} -\lambda(R_sL_r + R_rL_s) + j\omega_r & \lambda(R_r - jL_r\omega_r) \\ -R_s & 0 \end{bmatrix}$$

$$\boldsymbol{B} = \begin{bmatrix} \lambda L_r \\ 1 \end{bmatrix}$$

where R_s, R_r, L_s, L_r, and L_m are the stator resistance, rotor resistance, stator inductance, rotor inductance, and mutual inductance, respectively; ω_r is the rotor speed; and $\lambda = 1/\left(L_sL_r - L_m^2\right)$.

In digital implementation, (1) should be discretized to predict the torque and flux linkage at (k + 1)th instant. In this paper, the Heun's method [3] is employed to achieve a higher accuracy than the first-order Euler method. The discrete predictive equations of the IM are expressed as

$$\begin{bmatrix} \boldsymbol{i}_{sp}^{k+1} \\ \boldsymbol{\psi}_{sp}^{k+1} \end{bmatrix} = \begin{bmatrix} \boldsymbol{i}_s^k \\ \boldsymbol{\psi}_s^k \end{bmatrix} + \boldsymbol{A}T_{sc}\begin{bmatrix} \boldsymbol{i}_s^k \\ \boldsymbol{\psi}_s^k \end{bmatrix} + \boldsymbol{B}T_{sc}\boldsymbol{u}_s^k \tag{2}$$

$$\begin{bmatrix} \boldsymbol{i}_s^{k+1} \\ \boldsymbol{\psi}_s^{k+1} \end{bmatrix} = \begin{bmatrix} \boldsymbol{i}_{sp}^{k+1} \\ \boldsymbol{\psi}_{sp}^{k+1} \end{bmatrix} + \boldsymbol{A}\frac{T_{sc}}{2}\left(\begin{bmatrix} \boldsymbol{i}_{sp}^{k+1} \\ \boldsymbol{\psi}_{sp}^{k+1} \end{bmatrix} - \begin{bmatrix} \boldsymbol{i}_s^k \\ \boldsymbol{\psi}_s^k \end{bmatrix}\right) \tag{3}$$

where T_{sc} is the control period; $\boldsymbol{i}_{sp}^{k+1}$ and $\boldsymbol{\psi}_{sp}^{k+1}$ are the predictor–corrector of state variables; and $\boldsymbol{i}_s^{k+1}$ and $\boldsymbol{\psi}_s^{k+1}$ are the predicted state variables at (k + 1)th instant.

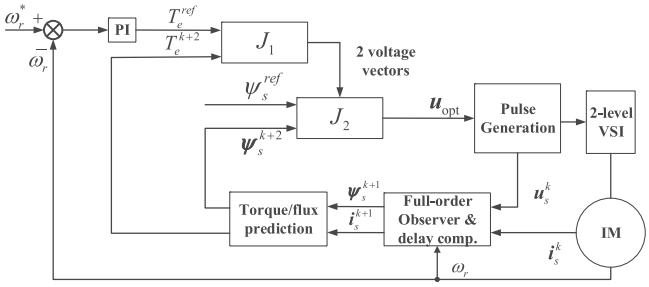

Fig. 1. Control diagram of the conventional SMPC.

III. Principle of the Proposed Method

The control diagrams of the conventional SMPC [13] and the proposed GSMPC are illustrated in Figs. 1 and 2, respectively. It is seen that both methods share the common parts of full-order observer, delay compensation, and torque/flux-linkage prediction. However, there are two noticeable differences between the two methods. First, in the conventional SMPC, the torque reference T_e^{ref} is obtained through an external speed control loop using the proportional-integral (PI) controller and the reference of stator flux linkage ψ_s^{ref} is set to a rated value ψ_s^{rated}. In the proposed GSMPC, as FW operation is considered, the torque

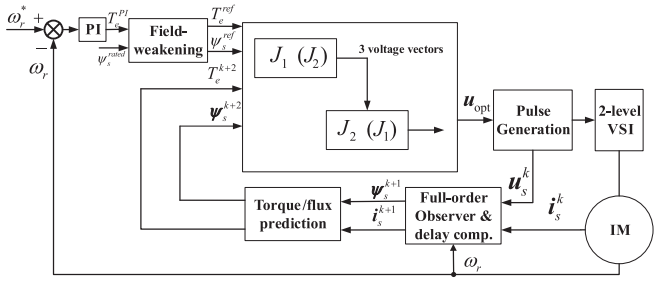

Fig. 2. Control diagram of the proposed GSMPC.

output T_e^{PI} from the PI controller and the rated stator flux linkage ψ_s^{rated} are sent to the FW block to obtain new references of the torque and stator flux linkage. This block only works when the rotor speed is above the rated speed and passes through the value of T_e^{PI} and ψ_s^{rated} when the motor speed is below the rated speed. Second, in the conventional SMPC, J_1 and J_2 denote the cost function of the torque error and flux linkage error and their execution order cannot be changed. Contrary to this, in the proposed GSMPC, there is no such limitation on the execution order of J_1 and J_2. As a result, two alternative methods exist and they are denoted as part 1 and part 2 in Fig. 2. The details of each block in Fig. 2 are introduced in the following texts.

A. Estimation and Prediction of Flux Linkage and Torque

In order to accurately estimate the stator flux linkage, a full-order observer based on the mathematical model of the IM in (1) is adopted in this paper and it is expressed as

$$\frac{\mathrm{d}\hat{\boldsymbol{x}}}{\mathrm{d}t} = \boldsymbol{A}\hat{\boldsymbol{x}} + \boldsymbol{B}\boldsymbol{u}_s + \boldsymbol{G}(\boldsymbol{i}_s - \hat{\boldsymbol{i}}_s) \tag{4}$$

where $\hat{\boldsymbol{x}} = [\,\hat{\boldsymbol{i}}_s \;\; \hat{\boldsymbol{\psi}}_s\,]^T$ are state variables representing the estimated stator current and stator flux linkage. A constant gain matrix $\boldsymbol{G}$ proposed in [19] is employed and it is expressed as

$$\boldsymbol{G} = -\begin{bmatrix} 2b \\ b/(\lambda L_r) \end{bmatrix} \tag{5}$$

where b is a negative constant. More details about this observer can be found in [19].

After obtaining the estimated stator flux linkage $\boldsymbol{\psi}_s^k$ from (4), the stator current $\boldsymbol{i}_s^{k+1}$ and stator flux linkage $\boldsymbol{\psi}_s^{k+1}$ at (k + 1)th instant can be predicted from (2) and (3) with $\boldsymbol{u}_s^k$ determined in the last control period as input. This step compensates the one-step delay in digital implementation [20].

In MPC for IM drives, the electromagnetic torque and stator flux linkage at (k + 2)th instant should be predicted for a given voltage vector after the one-step delay compensation. The torque is predicted as

$$T_e^{k+2} = \frac{3}{2}N_p(\boldsymbol{\psi}_s^{k+2} \otimes \boldsymbol{i}_s^{k+2}) \tag{6}$$

where N_p is the number of pole pairs and $\otimes$ represents cross product of two complex vectors. It is seen from (6) that both the information of $\boldsymbol{\psi}_s^{k+2}$ and $\boldsymbol{i}_s^{k+2}$ are required. The stator flux linkage can be simply predicted from the stator voltage equation, as shown in the second row of (1). However, the prediction of the stator current is relatively complicated. As the stator current is not directly used in the cost function of MPC, the torque at (k + 2)th instant can be calculated without the prediction of the stator current $\boldsymbol{i}_s^{k+2}$, which is expressed as [6]

$$T_e^{k+2} = \frac{3}{2}N_p(\boldsymbol{\psi}_s^{k+2} \otimes \boldsymbol{i}_{s0}^{k+1}). \tag{7}$$

The calculation of $\boldsymbol{i}_{s0}^{k+1}$ is only related to the variables at $k+1$ instant and it is expressed as

$$\begin{aligned}\boldsymbol{i}_{s0}^{k+1} = {} & (1 - \lambda R_s L_s T_{sc} + j\omega_r T_{sc})\boldsymbol{i}_s^{k+1} \\ & + \lambda(R_r T_{sc} - L_r - j\omega_r L_r T_{sc})\boldsymbol{\psi}_s^{k+1}.\end{aligned} \tag{8}$$

By using (7) and (8), only the prediction of the stator flux linkage is necessary and the relatively complicated prediction of the stator current is avoided, which reduces the computational burden. After obtaining $\boldsymbol{i}_s^{k+1}$ and $\boldsymbol{\psi}_s^{k+1}$ based on (2) and (3), the stator flux at (k + 2)th instant can be calculated as

$$\boldsymbol{\psi}_s^{k+2} = \boldsymbol{\psi}_s^{k+1} + T_{sc}(\boldsymbol{u}_s^{k+1} - R_s\boldsymbol{i}_s^{k+1}). \tag{9}$$

B. Principle of FW Operation

Operation in high speeds above the rated speed is important for IM drives in various industry applications. Introducing FW operation into MPC further improves its practical value. In this paper, a new FW method is proposed by adjusting the torque reference and stator flux linkage reference online.

The stator flux linkage reference is such designed that, when the rotor speed is above the rated speed, it is inversely proportional to the rotor speed, as follows:

$$\psi_s^{\mathrm{ref}} = \psi_s^{\mathrm{rated}} \times \frac{\omega_{\mathrm{rated}}}{\omega_r} \tag{10}$$

where ω_{rated} is the rated speed of the machine.

It has been shown in [15] that for a stator flux linkage oriented system, the simple $1/\omega_r$ method produces nearly optimal torque capability over the entire speed range. However, it is not known whether the maximum load angle of 45°, which is the angle between the stator flux linkage vector and the rotor flux linkage vector, has been achieved. In fact, to obtain the maximum torque ability during the FW operation, apart from the change on the flux linkage reference, the torque reference should also be appropriately bounded. In other words, the accurate torque limitation should be known.

To limit the stator current exceeding the rated value, the maximum torque reference should be accordingly adjusted with the stator flux linkage reference as

$$T_{m1} = T_{\mathrm{rated}} \times \frac{\psi_s^{\mathrm{ref}}}{\psi_s^{\mathrm{rated}}} = T_{\mathrm{rated}} \times \frac{\omega_{\mathrm{rated}}}{\omega_r} \tag{11}$$

where T_{rated} is the rated torque of the machine.

The relationship between the stator flux and rotor flux is [19]

$$\frac{d\boldsymbol{\psi}_r}{dt} + (\lambda L_s R_r - j\omega_r)\,\boldsymbol{\psi}_r = \lambda L_m R_r \boldsymbol{\psi}_s. \tag{12}$$

Under steady state, (12) is simplified as

$$\boldsymbol{\psi}_r = \frac{\lambda L_m R_r}{\lambda L_s R_r + j\omega_{\mathrm{sl}}}\boldsymbol{\psi}_s \tag{13}$$

where $\omega_{\rm sl}$ is the slip speed.

According to (13), the electromagnetic torque can be calculated as

$$\begin{aligned} T_e &= \frac{3}{2}N_p\lambda L_m \,\mathrm{Im}\left(\boldsymbol{\psi}_r^* \boldsymbol{\psi}_s\right) \\ &= \frac{3}{2}N_p\lambda L_m \,\mathrm{Im}\left(\frac{\lambda L_m R_r}{\lambda L_s R_r - j\omega_{\rm sl}}\right)|\boldsymbol{\psi}_s|^2 \\ &= \frac{3}{2}N_p\left(\lambda L_m\right)^2 R_r \frac{\omega_{sl}}{\left(\lambda L_s R_r\right)^2 + \omega_{\rm sl}^2}|\boldsymbol{\psi}_s|^2 \end{aligned} \tag{14}$$

where Im(•) means the imaginary part of a complex vector. When the following equation is true

$$\omega_{\rm sl} = \lambda L_s R_r \tag{15}$$

T_e expressed in (14) could reach its maximum value as

$$T_{e\max} = \frac{3}{4}N_p\lambda\frac{L_m^2}{L_s}|\boldsymbol{\psi}_s|^2 \tag{16}$$

The resulting maximum torque in (16) is the same as the expression in [18] and [21] but derived in a different way. Submitting (15) into (13), the relationship between the rotor flux linkage vector and stator flux linkage vector is obtained as

$$\boldsymbol{\psi}_r = \frac{L_m/L_s}{1+j}\boldsymbol{\psi}_s = \frac{1}{\sqrt{2}}\frac{L_m}{L_s}e^{-j\frac{\pi}{4}}\boldsymbol{\psi}_s. \tag{17}$$

From (17), it is clearly seen that the rotor flux linkage vector should lag the stator flux linkage vector by 45° to achieve the theoretical maximum torque. As the rotor flux linkage is not the control variable in this paper, it is more convenient to express the maximum torque in terms of the stator current and stator flux linkage for the proposed method.

According to the model of IM, the stator current can be calculated from the stator flux and rotor flux as

$$\boldsymbol{i}_s = \lambda\left(L_r\boldsymbol{\psi}_s - L_m\boldsymbol{\psi}_r\right). \tag{18}$$

Substituting (17) into (18), the relationship between stator current and stator flux linkage can be obtained as

$$\boldsymbol{i}_s = \lambda\frac{L_rL_s - L_m^2 + jL_rL_s}{L_s(1+j)}\boldsymbol{\psi}_s. \tag{19}$$

Considering the leakage inductance is usually much smaller than the self-inductance, it is reasonable to assume that $L_rL_s - L_m^2 \approx 0$, which simplifies (19) as

$$\boldsymbol{i}_s = \lambda L_r\frac{1}{\sqrt{2}}e^{j\frac{\pi}{4}}\boldsymbol{\psi}_s \tag{20}$$

which means that the stator current should lead the stator flux linkage by 45° to achieve the maximum torque.

According to (7) and (20), the maximum torque reference should be limited to

$$T_{m2} = \frac{3\sqrt{2}}{4}N_p|\boldsymbol{i}_{s0}|\psi_s^{\rm ref} \tag{21}$$

where $\boldsymbol{i}_{s0}$ can be calculated according to (8).

Combining (11) and (21), the torque reference should be finally set as

$$T_e^{\rm ref} = \min(T_e^{\rm PI},\ T_{m1},\ T_{m2}). \tag{22}$$

It should be noted that if $T_e^{\rm PI}$ is negative, which means the rotor speed is above the reference speed, in that case the torque reference should be limited as

$$T_e^{\rm ref} = \max(T_e^{\rm PI},\ -T_{m1},\ -T_{m2}) \tag{23}$$

By using (10), (22), or (23), both the reference value of the stator flux linkage and torque are adjusted online, which help to achieve optimal torque ability when the speed is higher than the rated speed.

C. Optimal Vector Selection

In the conventional MPC for IM drives, the cost function is usually defined as the combination of the torque error and flux linkage error [3], [22], as follows:

$$J = |T_e^{\rm ref} - T_e^{k+2}| + k_\psi|\psi_s^{\rm ref} - |\boldsymbol{\psi}_s^{k+2}|| \tag{24}$$

where $T_e^{\rm ref}$ and $\psi_s^{\rm ref}$ are the references of the torque and stator flux linkage amplitude, and k_ψ is a weighting factor for the stator flux linkage. As the torque and stator flux linkage have different amplitude and units, k_ψ needs to be carefully tuned to achieve the satisfactory performance, which is usually a tedious work.

In the conventional SMPC, the use of a single cost function in (24) is abandoned and two separate cost functions are used, which are expressed as

$$J_1 = |T_e^{\rm ref} - T_e^{k+2}| \tag{25}$$

$$J_2 = |\psi_s^{\rm ref} - |\boldsymbol{\psi}_s^{k+2}||. \tag{26}$$

As shown in Fig. 1, the cost function J_1 for the torque error is first evaluated for each voltage vector. The two voltage vectors producing smaller torque error than other vectors are selected, and then, sent to the second cost function J_2 for the flux linkage error. The one producing the minimal flux linkage error is selected as the final optimal voltage vector. The cascaded evaluation of different cost functions provides a way to eliminate the weighting factor. However, it is not analyzed how many candidate vectors should be selected from the first cost function. Furthermore, the feasibility of exchanging the execution order of J_1 and J_2 is not discussed. In fact, if J_2 is first evaluated to select two voltage vectors, and then, J_1 is evaluated, it is found that the system cannot achieve stable operation over the full speed range, as shown in Fig. 3(b). Thus, the conventional SMPC should be improved so that it can work stably under different conditions.

The proposed GSMPC inherits the cascaded structure of two cost functions in the conventional SMPC. However, when evaluating the first cost function for torque, three rather than two vectors are selected, which produce a smaller torque error than other vectors. Thus, the candidate vectors to be evaluated in the second cost function of the flux linkage error increase from two to three. Although the computational burden may be slightly increased, there are various benefits and advantages in the proposed GSMPC. On one hand, the proposed GSMPC achieves better balance between the torque control and flux control, leading to a reduction in the current harmonics and total harmonic

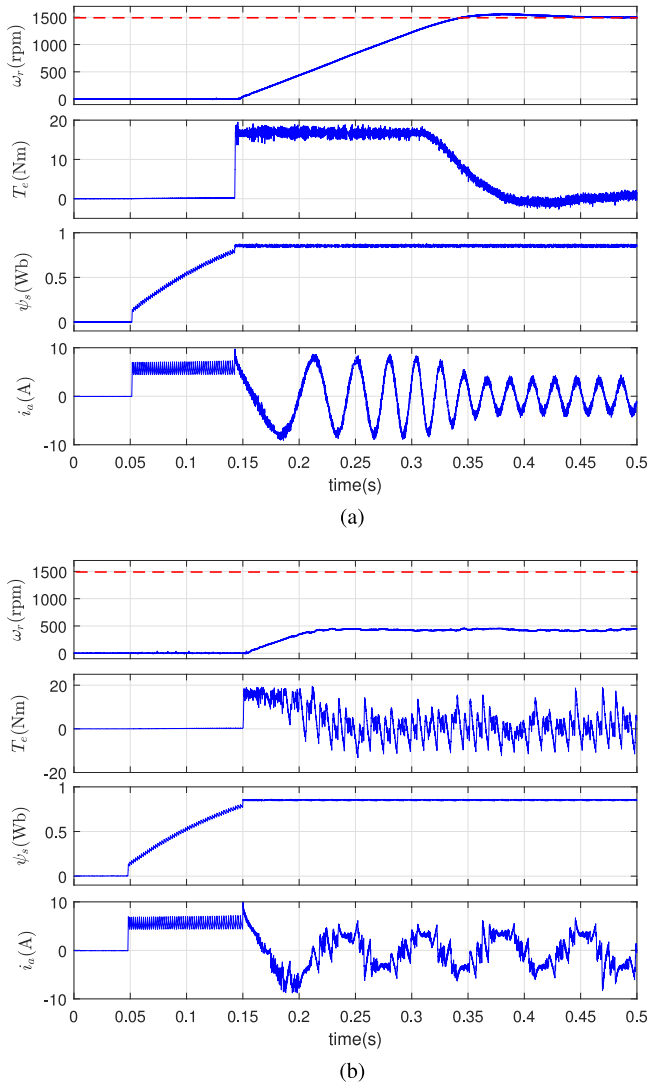

Fig. 3. Starting response from standstill to 1500 r/min for (a) SMPC_T_e and (b) SMPC_ψ_s.

distortion (THD). On the other hand, the proposed GSMPC does not have limitation on the execution order of J_1 and J_2. Contrary to the conventional SMPC, which cannot work if J_2 is first evaluated, the proposed method can work effectively whether J_1 or J_2 is first evaluated, as shown in Part 1 and Part 2 in Fig. 2. This greatly improves the universality of the system.

It should be noted that selecting more than three vectors from the first function generally means lower priority for the variable in the first cost function. For an extreme case, where seven voltage vectors are selected in the first cost function of the conventional SMPC, the system loses the ability for torque control and only stator flux linkage control is achieved. In fact, according to our study, for the conventional SMPC, selecting two or three vectors from the first cost function for the torque, both works. However, if the cost function for the stator flux linkage is first evaluated, the system only works when three, four, or five vectors are selected. Due to page limitations, these results are not shown and only the conclusion is summarized here. It can be seen that selecting three vectors is effective for both cases. That is why the proposed GSMPC selects three vectors rather than two vectors for the first cost function.

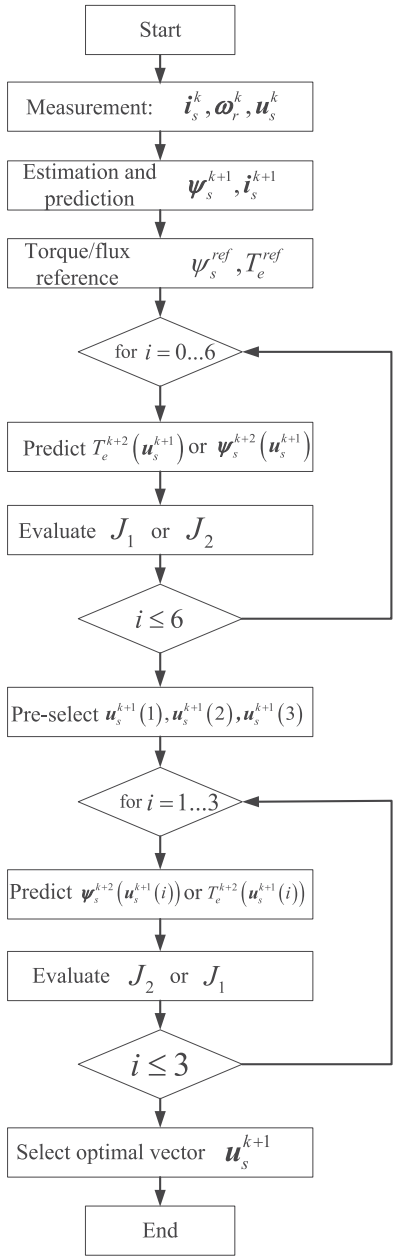

Fig. 4. Flow diagram of the proposed GSMPC.

The flowchart of the proposed GSMPC is shown in Fig. 4 and the procedure of the GSMPC is briefly summarized as follows.

1) Obtain i_s^k and ω_r^k from measurement, and reconstruct the optimal voltage vector u_s^k in the previous control period.
2) Estimate the stator flux linkage at (k)th instant from (4), and compensate the one-step delay using (2) and (3) to predict the stator flux linkage vector $\boldsymbol{\psi}_s^{k+1}$ and stator current $\boldsymbol{i}_s^{k+1}$ at $k+1$ instant.
3) Calculate the torque output from the PI controller, and then, obtain the final reference value of the torque and stator flux linkage using the FW strategy according to (10), (22), or (23).

TABLE I
MACHINE AND CONTROL PARAMETERS

DC-bus voltage	U_{dc}	540 V
Rated power	P_N	2.2 kW
Rated voltage	U_N	380 V
Rated frequency	f_N	50 Hz
Rated torque	T_N	14 Nm
Number of pole pairs	N_p	2
Stator resistance	R_s	3.065 Ω
Rotor resistance	R_r	1.879 Ω
Mutual inductance	L_m	0.232 H
Stator inductance	L_s	0.242 H
Rotor inductance	L_r	0.242 H
Flux linkage reference	ψ_s^{ref}	0.85 Wb-turns

4) Predict torque and stator flux linkage at (k + 2)th instant according to (7) and (9).
5) Evaluate the first cost function J_1 (J_2) for each converter voltage vector and select three vectors producing smaller value of the cost function than other vectors.
6) Evaluate the second cost function J_2 (J_1) for the three vectors obtained from the first cost function.
7) Select the optimal voltage vector minimizing the second cost function and apply it in the next control period.

IV. SIMULATION STUDY

To confirm the effectiveness of the proposed GSMPC, simulation study is carried out in the environment of MATLAB/Simulink with a sampling frequency of 15 kHz. The study of the impact resulted from parameter mismatches on MPC is beyond the scope of this paper. It is assumed that model parameters are known with good accuracy in the following tests. If there are uncertainties in the model parameters, the methods presented in [23] and [24] could be used to improve the parameter robustness. The machine and control parameters are listed in Table I. The conventional SMPC in [13] is also presented for the aim of comparison. In the following parts, the original SMPC evaluating the cost function of the torque first is called SMPC_T_e and the one evaluating the cost function of the stator flux linkage first is called SMPC_ψ_s. In a similar way, the proposed GSMPC evaluating the cost function of the torque first is called GSMPC_T_e and the one evaluating the cost function of stator flux linkage first is called GSMPC_ψ_s.

Fig. 5 illustrates the starting response from standstill to 1500 r/min for SMPC_T_e and SMPC_ψ_s. From top to bottom, the curves shown in Fig. 5 are rotor speed, electromagnetic torque, stator flux linkage amplitude, and one phase stator current. The stator flux linkage is first established following the way in [19] by injecting a dc current into the machine to provide the sufficient starting torque without large current. It is seen that in SMPC_T_e, the motor accelerates quickly to 1500 r/min with the maximum torque when the stator flux has been established. On the contrary, in SMPC_ψ_s, the motor only runs to less than 500 r/min, which is far from the reference speed of 1500 r/min. Although the stator flux linkage is well controlled, there are large oscillations in the torque and significant harmonics in the stator current. The possible reason for the failure in SMPC_ψ_s is that only two vectors are selected as candidate vectors for the minimization of the torque error in the second cost function, which may exclude the vectors useful for the torque control. The simulation results prove that the conventional SMPC only works under some special cases and is not a universal method.

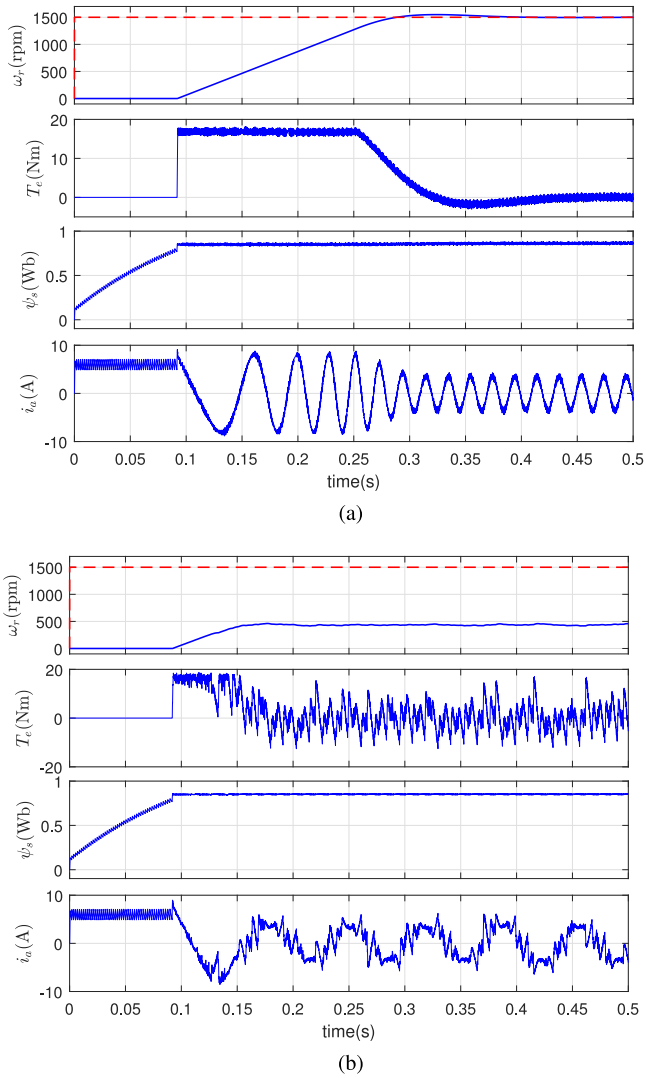

Fig. 5. Simulated starting response from standstill to 1500 r/min for (a) SMPC_T_e and (b) SMPC_ψ_s.

The simulation results obtained from GSMPC_T_e and GSMPC_ψ_s are illustrated in Fig. 6. It is seen that both methods achieve a fast and stable starting process by presenting very similar response to that of SMPC_T_e. This proves that the proposed GSMPC is more universal than the conventional SMPC by eliminating the limitation on the execution order of two cost functions in MPC. One of the possible reasons is that the proposed GSMPC selects three instead of two vectors for the second cost function to evaluate, which can achieve better balance between torque control and stator flux control. The simulation results are confirmed by the experimental results in Section V.

V. EXPERIMENTAL RESULTS

Apart from the simulation study, experimental tests from a 2.2- kW laboratory IM drive system are also carried out to

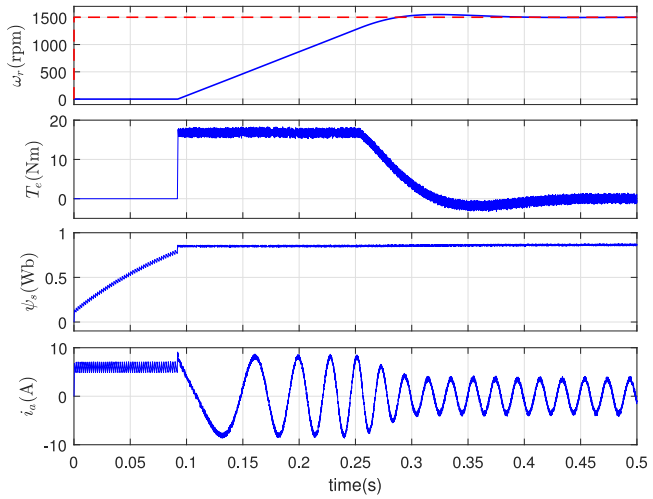

(a)

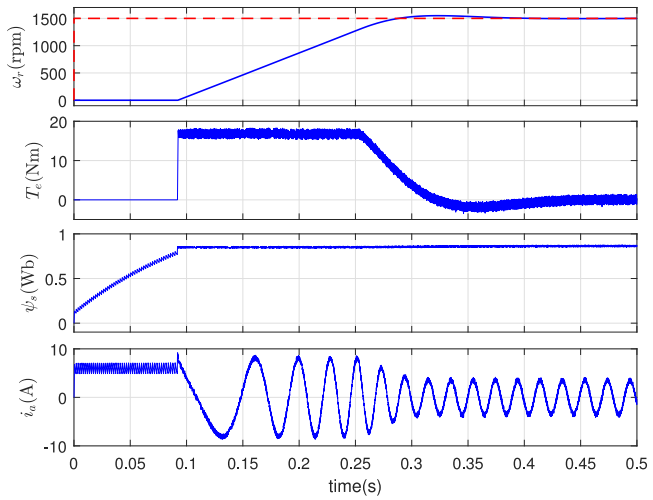

(b)

Fig. 6. Simulated starting response from standstill to 1500 r/min for (a) GSMPC_T_e and (b) GSMPC_ψ_s.

confirm the theoretical study and the effectiveness of the proposed method. The experimental setup is illustrated in Fig. 7, where a magnetic powder brake coupled to the shaft of the IM is employed to apply load torque. A 32-bit floating point DSP TMS320F28335 is used to implement the conventional SMPC and the proposed GSMPC. The torque waveform illustrated in the experimental tests is the result calculated according to (6). The rotor speed is measured with a 2000-pulses-per-revolution optical-type encoder. The conventional MPC [1] that employs a single cost function takes 49.3826 μs to accomplish the whole algorithm, while it takes 58.5133 μs for the prior SMPC_T_e. For the proposed methods, if FW operation is not considered, the execution time are 58.9333 and 58.9067 μs for GSMPC_T_e and GSMPC_ψ_s respectively. The execution time of the prior SMPC and the proposed GSMPC is longer because of the additional sorting algorithm required to select the optimal voltage vector from the evaluation of the first and the second cost functions. However, the execution time of the GSMPC is almost the same with that of the SMPC. In other words, selecting three instead of

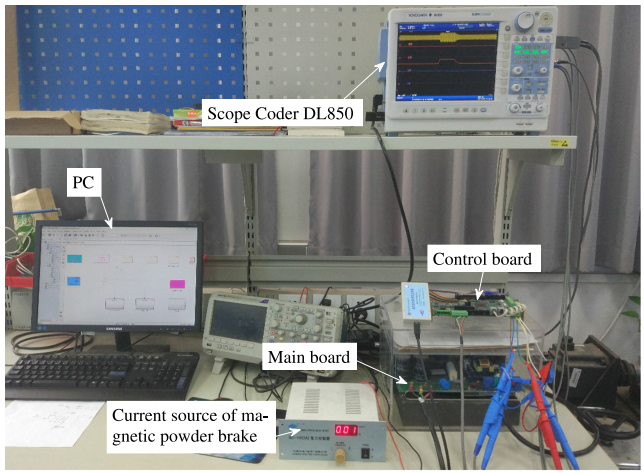

(a)

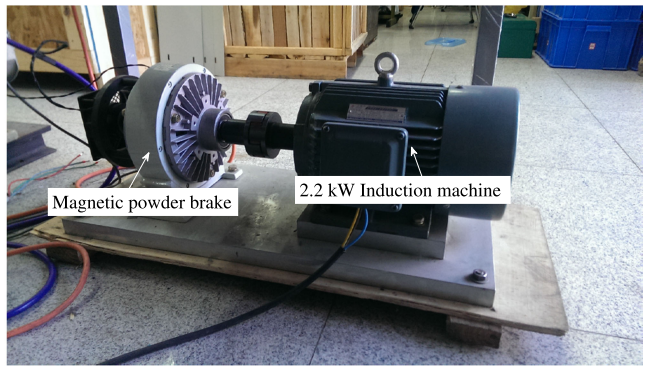

(b)

Fig. 7. Experimental setup of a two-level inverter-fed IM drive. (a) Inverter and oscilloscope. (b) 2.2-kW IM and magnetic powder brake.

two vectors from the first cost function only slightly increases the computational burden, but brings the benefits of less flux linkage ripples and current THD, as shown in the testing results. The motor parameters have been listed in Table I and the sampling frequency is 15 kHz for each method, which is the same as that in the simulation part. In the following tests, all the displayed variables are obtained via a 12-bit on-board digital to analog converter DAC7724U, except the stator current, which is directly measured by a current probe. All data are recorded using an oscilloscope DL850E, and then, transferred to the PC for analysis and plotting.

A. *Dynamic Response*

First, the dynamic response of starting from standstill to 1500 r/min is tested for both conventional SMPC and the proposed GSMPC, as shown in Figs. 3 and 8. It is seen from Fig. 3 that SMPC_T_e works effectively, while SMPC_ψ_s can only run to the speed of less than 500 r/min with significant torque oscillations and current harmonics, which is in accordance to the simulation results in Fig. 5. On the contrary, both GSMPC_T_e and GSMPC_ψ_s presents similar dynamic response to that of SMPC_T_e. After establishing the stator flux using pre-excitation, the machine accelerates quickly to the reference speed with the maximum torque without large starting

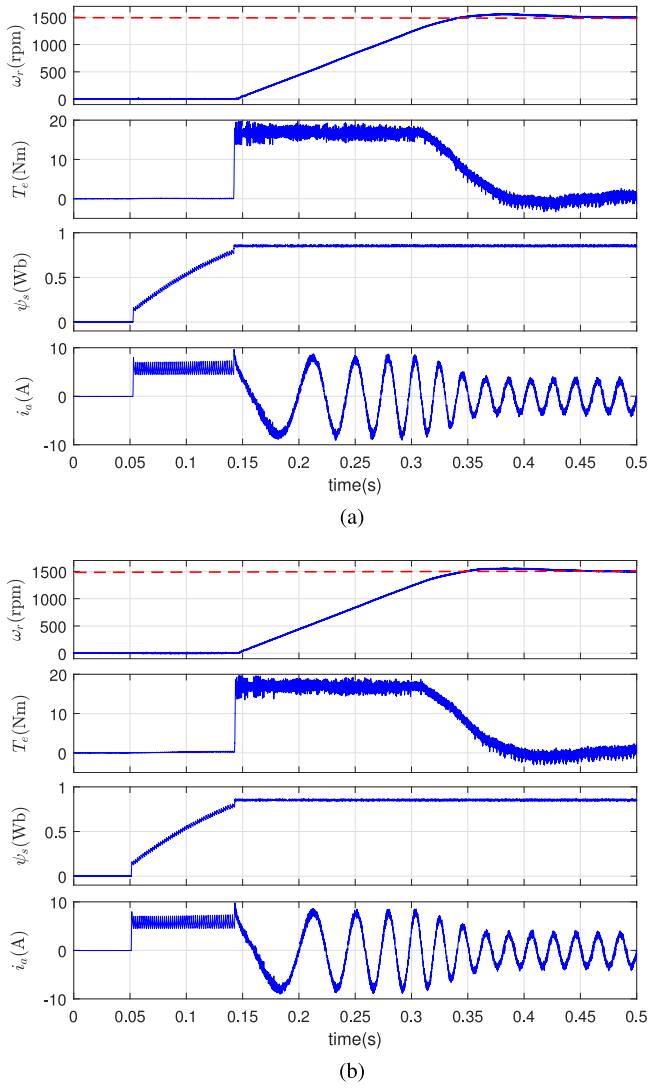

Fig. 8. Starting response from standstill to 1500 r/min for (a) GSMPC_T_e and (b) GSMPC_ψ_s.

current. Decoupled control of the torque and stator flux linkage is achieved in the two variants of the proposed GSMPC. The results confirm that the proposed GSMPC improves the universality of the conventional SMPC.

As SMPC_ψ_s fails to work, in the following parts, only the results obtained from SMPC_T_e, GSMPC_T_e, and GSMPC_ψ_s are presented. Fig. 9 presents the dynamic response of the speed reversal at $\pm$1500 r/min for each method. The machine first operates at 1500 r/min without load, and then, changes quickly to $-$1500 r/min with the maximum negative torque. During the dynamic process, decoupled torque control and flux linkage control is achieved for each method. For the conventional SMPC_T_e, as torque is assigned higher priority, there are less torque ripples than GSMPC_T_e and GSMPC_ψ_s. However, the flux linkage ripples of SMPC_T_e are higher than GSMPC_T_e and GSMPC_ψ_s. During the dynamic process, there are even short-time dip in the stator flux linkage amplitude for SMPC_T_e. The results confirm that the proposed GSMPC can achieve better balance between torque control and flux linkage control, while

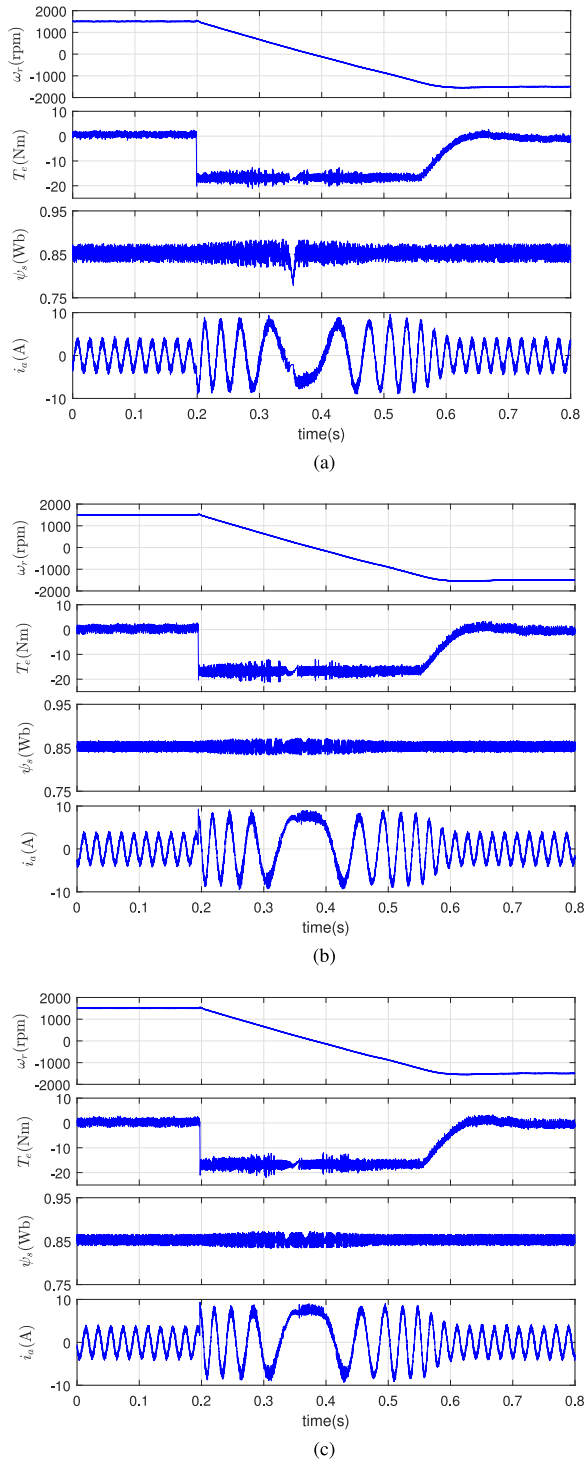

Fig. 9. Dynamic response of speed reversal at $\pm$1500 r/min for (a) SMPC_T_e, (b) GSMPC_T_e, and (c) GSMPC_ψ_s.

the conventional SMPC gives too much priority to the torque control.

B. Steady-State Performance

It can be seen from Figs. 3, 8, and 9 that the proposed GSMPC achieves similar dynamic response to the conventional SMPC. However, they differ in the steady-state performance in terms of

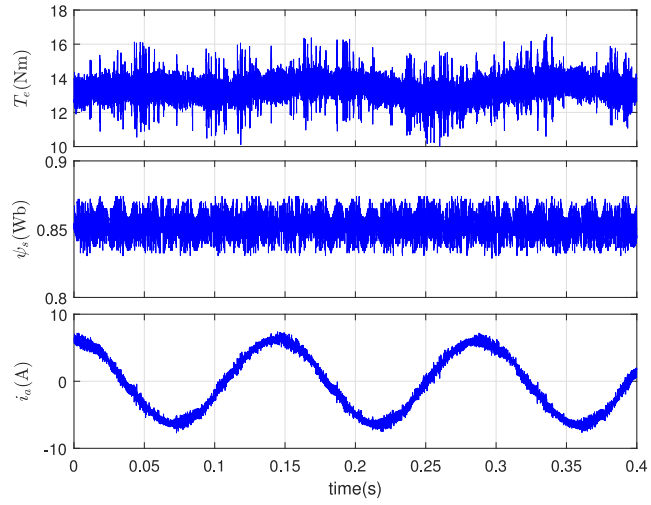

(a)

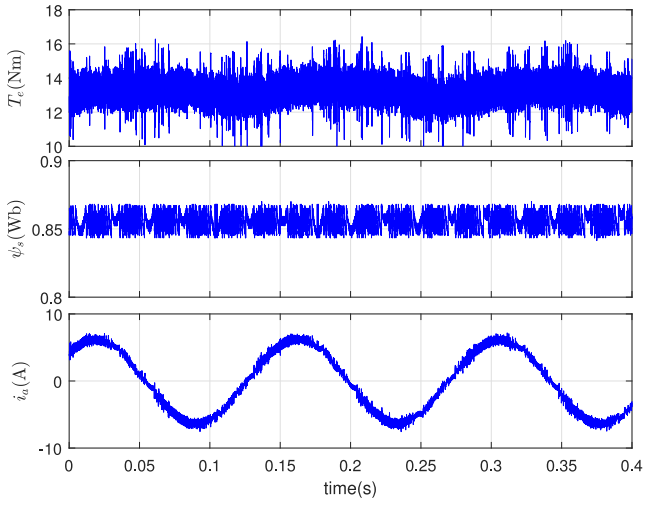

(b)

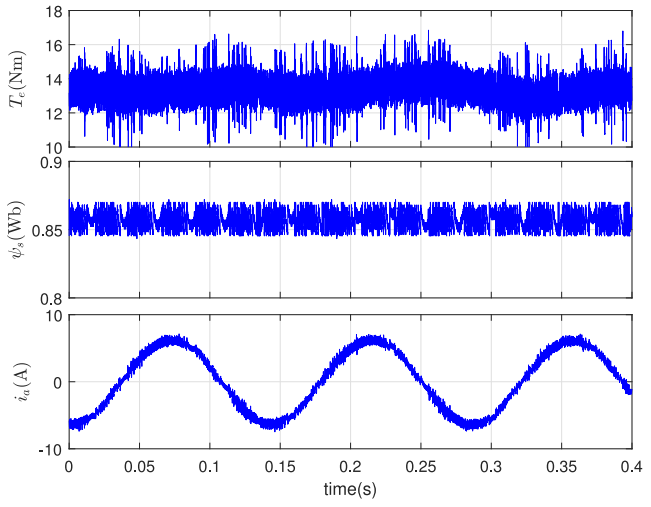

(c)

Fig. 10. Low-speed operation of 150 r/min with rated torque for (a) SMPC_T_e, (b) GSMPC_T_e, and (c) GSMPC_ψ_s.

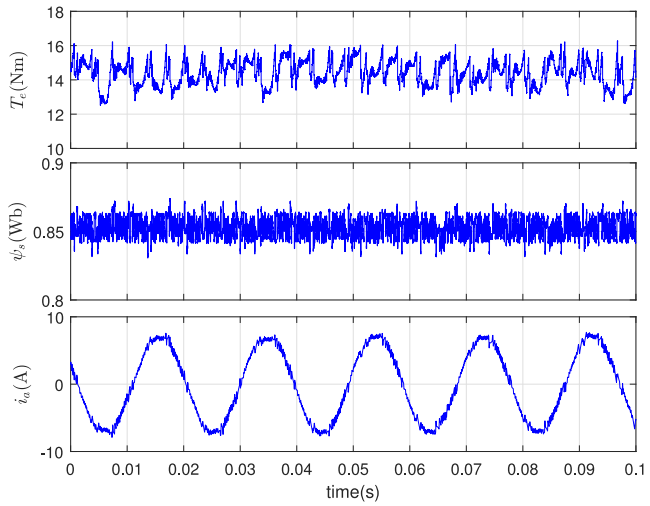

(a)

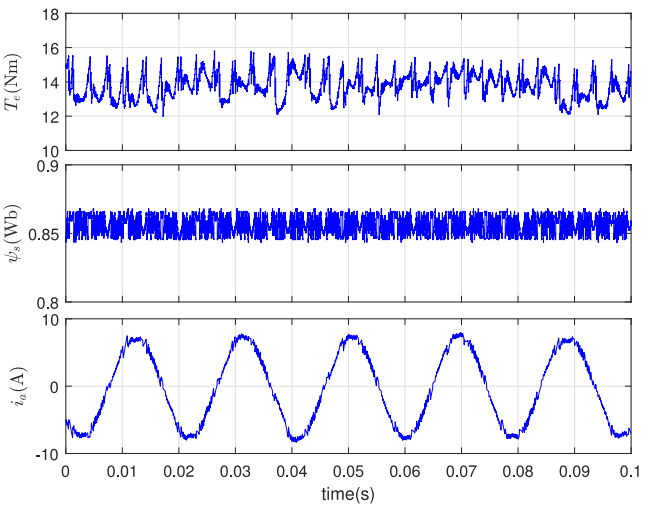

(b)

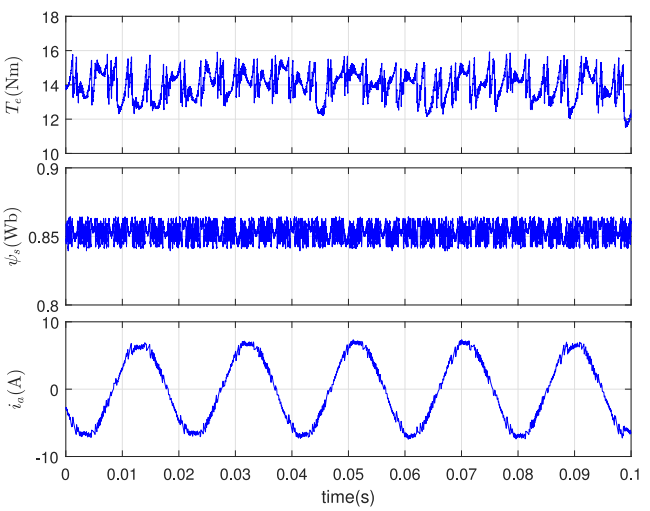

(c)

Fig. 11. High-speed operation of 1500 r/min with rated torque for (a) SMPC_T_e, (b) GSMPC_T_e, and (c) GSMPC_ψ_s.

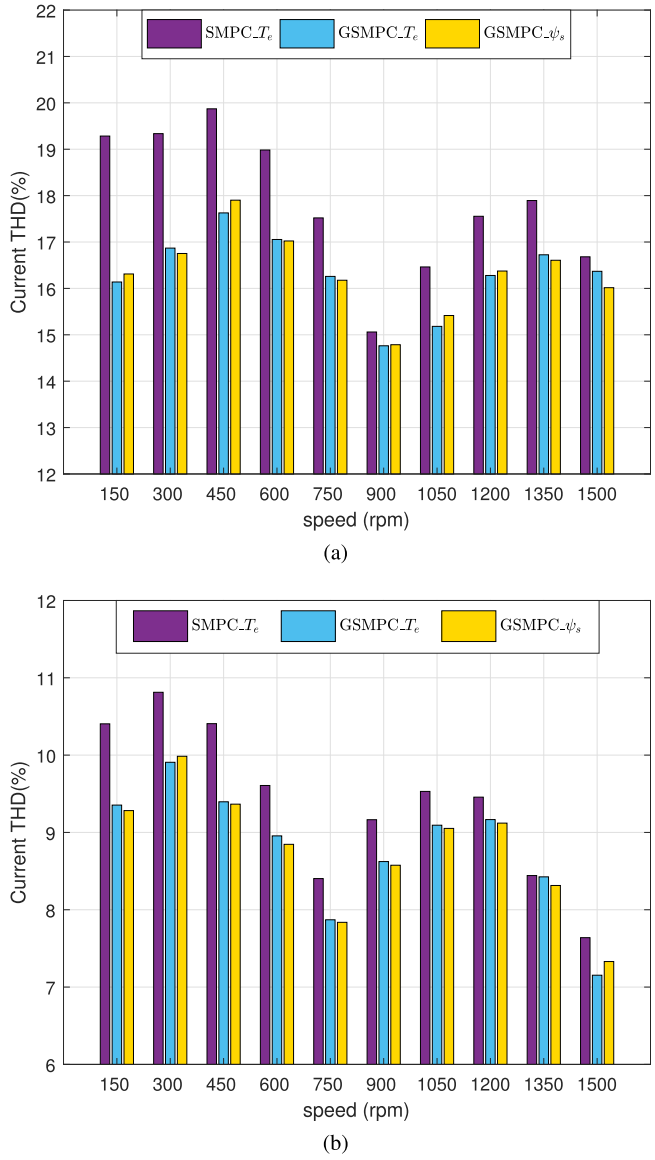

Fig. 12. Comparisons of current THD for SMPC_T_e, GSMPC_T_e, and GSMPC_ψ_s at different speeds. (a) Without load. (b) With rated load.

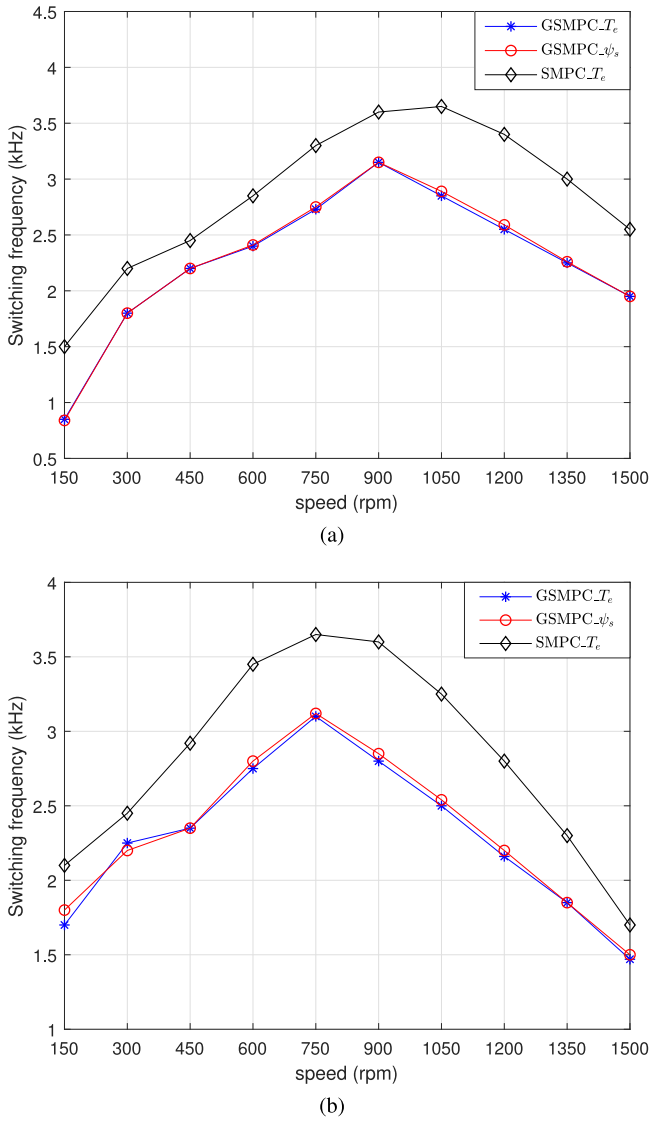

Fig. 13. Average switching frequencies for SMPC_T_e, GSMPC_T_e, and GSMPC_ψ_s at different speeds. (a) Without load. (b) With rated load.

torque/flux-linkage ripples and current harmonics. In this part, a detailed steady-state performance comparison of the conventional SMPC and the proposed GSMPC will be presented.

Fig. 10 presents the steady-state response at 150 r/min with rated torque for SMPC_T_e, GSMPC_T_e, and GSMPC_ψ_s. It is clearly seen that the conventional SMPC_T_e has lower torque ripples than those of GSMPC_T_e and GSMPC_ψ_s, but the flux linkage ripples are higher and more irregular. Similar results can be seen at high speed of 1500 r/min with rated torque, as shown in Fig. 11. Again it is seen that the proposed GSMPC performs better in terms of stator flux linkage ripples, while the conventional SMPC_T_e is better in terms of torque ripples. As three optimal vectors are selected for the second cost function, the proposed GSMPC achieves better balance between the torque control and flux linkage control. As a result, the proposed GSMPC not only presents lower flux linkage ripples, but the stator current THD is also lower than that of the conventional SMPC_T_e. This is confirmed in Fig. 12, where the current THDs for three methods at different speeds with and without load are presented. It is seen that, GSMPC_T_e and GSMPC_ψ_s have a lower current THD than that of SMPC_T_e at any speeds, while the performance difference between them is insignificant.

The average switching frequencies for SMPC_T_e, GSMPC_T_e, and GSMPC_ψ_s at different speeds are shown in Fig. 13. As only one voltage vector is applied during one control period, the three methods presents variable switching frequency, which is low at low and high speeds but high at medium speed. From Fig. 13, it can be seen that the average switching frequencies of GSMPC_T_e and GSMPC_ψ_s are almost the same at different speeds, which means that both methods achieve similar balance between torque control and flux linkage control. However, SMPC_T_e has higher switching frequency compared with the proposed GSMPC during the whole speed range under the same test conditions. As shown in Fig. 12, the proposed GSMPC presents a lower current THD. This implies there are

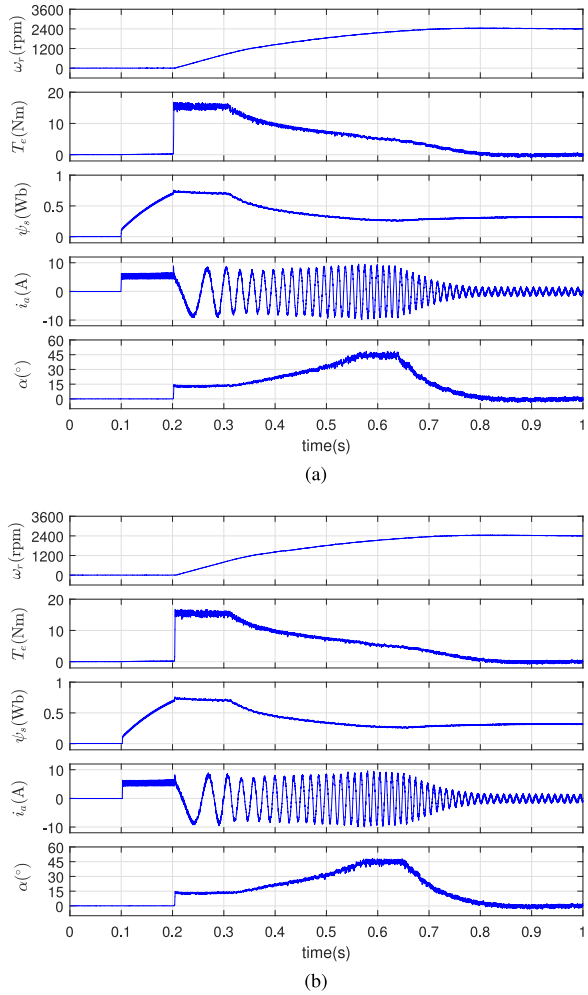

Fig. 14. Starting from standstill to 240% base speed with 66.7% dc bus voltage. (a) GSMPC_T_e. (b) GSMPC_ψ_s.

unnecessary switching actions in the prior SMPC, which can indirectly justify the superiority of the proposed method.

C. FW Operation

In this part, the proposed GSMPC is extended to the high-speed region above the base speed by introducing the FW technique introduced in Section III-B. For the sake of safety, the dc bus voltage is reduced to 66.7% of the rated value and the based speed is 1000 r/min. Fig. 14 presents the starting response from standstill to 240% base speed (2400 r/min) for both GSMPC_T_e and GSMPC_ψ_s. Very similar response can be observed in both methods. To clearly show the effectiveness of the proposed FW technique, the last curve in Fig. 14 is the load angle between the stator flux linkage and rotor flux linkage. Before the motor reaching the based speed of 1000 r/min, the motor accelerates quickly with rated torque, and then, the stator flux linkage amplitude decreases with the speed increase. The maximum load angle obtained in GSMPC_T_e and GSMPC_ψ_s are 44.15° and 44.38°, which are very close to the theoretical value of 45°. The results confirm that optimal torque ability is achieved when the proposed FW technique is combined with the GSMPC.

VI. Conclusion

The design of the weighting factor for MPC in IM drives has been a tedious and nontrivial work due to the lack of the theoretical guidance. The weighting factor can be eliminated in SMPC by evaluating the cost functions for the torque and stator flux linkage in a cascaded way. However, only two vectors selected from the cost function of the torque are evaluated in the second cost function of the stator flux linkage, which assigns too much priority to the torque control. It is shown in this paper that during the dynamic process, there are even dip in the stator flux linkage amplitude. Furthermore, if the cost function for the stator flux linkage is first evaluated, the system cannot work effectively and there are significant torque oscillations and current harmonics.

This paper proposes a GSMPC, which selects three other than two vectors when evaluating the first cost function. As a result, it achieves better balance between torque control and flux linkage control. The proposed GSMPC works effectively irrespective of the execution order of the cost function, which increases the universality of the conventional SMPC. Better steady-state performance than the conventional SMPC is achieved in the proposed GSMPC by presenting less stator flux linkage ripples and lower current THD. Furthermore, it is shown that with the same sampling frequency, the proposed GSMPC has even lower average switching frequency in the entire speed range.

The proposed GSMPC is further enhanced by introducing a simple FW technique, which only requires to change the reference value of the stator flux linkage and torque online. The experimental results prove that the system works steadily at 240% base speed and the theoretical maximum load angle of 45° is closely reached.

References

[1] H. Miranda, P. Cortes, J. Yuz, and J. Rodriguez, "Predictive torque control of induction machines based on state-space models," *IEEE Trans. Ind. Electron.*, vol. 56, no. 6, pp. 1916–1924, Jun. 2009.

[2] S. Vazquez *et al.*, "Model predictive control: A review of its applications in power electronics," *IEEE Ind. Electron. Mag.*, vol. 8, no. 1, pp. 16–31, Mar. 2014.

[3] Y. Zhang, H. Yang, and B. Xia, "Model-predictive control of induction motor drives: Torque control versus flux control," *IEEE Trans. Ind. Appl.*, vol. 52, no. 5, pp. 4050–4060, Sep. 2016.

[4] P. Cortes *et al.*, "Guidelines for weighting factors design in model predictive control of power converters and drives," in *Proc. IEEE Int. Conf. Ind. Technol.*, 2009, pp. 1–7.

[5] C. Rojas, J. Rodriguez, F. Villarroel, J. Espinoza, C. Silva, and M. Trincado, "Predictive torque and flux control without weighting factors," *IEEE Trans. Ind. Electron.*, vol. 60, no. 2, pp. 681 –690, Feb. 2013.

[6] Y. Zhang and H. Yang, "Model predictive torque control of induction motor drives with optimal duty cycle control," *IEEE Trans. Power Electron.*, vol. 29, no. 12, pp. 6593–6603, Dec. 2014.

[7] S. Davari, D. Khaburi, and R. Kennel, "An improved FCS-MPC algorithm for an induction motor with an imposed optimized weighting factor," *IEEE Trans. Power Electron.*, vol. 27, no. 3, pp. 1540 –1551, Mar. 2012.

[8] C. A. Rojas, J. R. Rodriguez, S. Kouro, and F. Villarroel, "Multiobjective fuzzy-decision-making predictive torque control for an induction motor drive," *IEEE Trans. Power Electron.*, vol. 32, no. 8, pp. 6245–6260, Aug. 2017.

[9] F. Villarroel, J. Espinoza, C. Rojas, J. Rodriguez, M. Rivera, and D. Sbarbaro, "Multiobjective switching state selector for finite-states model predictive control based on fuzzy decision making in a matrix converter," *IEEE Trans. Ind. Electron.*, vol. 60, no. 2, pp. 589–599, Feb. 2013.

[10] Y. Zhang, Y. Bai, and H. Yang, "A universal multiple-vector-based model predictive control of induction motor drives," *IEEE Trans. Power Electron.*, vol. 33, no. 8, pp. 6957–6969, Aug. 2018.
[11] T. Geyer, "Algebraic weighting factor selection for predictive torque and flux control," in *Proc. IEEE Energy Convers. Congr. Expo.*, Oct. 2017, pp. 357–364.
[12] Y. Zhang and H. Yang, "Two-vector-based model predictive torque control without weighting factors for induction motor drives," *IEEE Trans. Power Electron.*, vol. 31, no. 2, pp. 1381–1390, Feb. 2016.
[13] M. Norambuena, J. Rodriguez, Z. Zhang, F. Wang, C. Garcia, and R. Kennel, "A very simple strategy for high-quality performance of ac machines using model predictive control," *IEEE Trans. Power Electron.*, vol. 34, no. 1, pp. 794–800, Jan. 2019.
[14] J. Su, R. Gao, and I. Husain, "Model predictive control based field-weakening strategy for traction EV used induction motor," *IEEE Trans. Ind. Appl.*, vol. 54, no. 3, pp. 2295–2305, May 2018.
[15] X. Xu and D. W. Novotny, "Selection of the flux reference for induction machine drives in the field weakening region," *IEEE Trans. Ind. Appl.*, vol. 28, no. 6, pp. 1353–1358, Nov. 1992.
[16] Y. Zhang, Y. Bai, H. Yang, and B. Zhang, "Low switching frequency model predictive control of three-level inverter-fed IM drives with speed sensorless and field-weakening operation," *IEEE Trans. Ind. Electron.*, to be published.
[17] H. Yang, Y. Zhang, P. D. Walker, J. Liang, N. Zhang, and B. Xia, "Speed sensorless model predictive current control with ability to start a free running induction motor," *IET Elect. Power Appl.*, vol. 11, no. 5, pp. 893–901, 2017.
[18] L. Zarri, M. Mengoni, A. Tani, G. Serra, D. Casadei, and J. O. Ojo, "Control schemes for field weakening of induction machines: A review," in *Proc. IEEE Workshop Elect. Mach. Des., Control Diagnosis*, Mar. 2015, pp. 146–155.
[19] Y. Zhang, J. Zhu, Z. Zhao, W. Xu, and D. Dorrell, "An improved direct torque control for three-level inverter-fed induction motor sensorless drive," *IEEE Trans. Power Electron.*, vol. 27, no. 3, pp. 1502 –1513, Mar. 2012.
[20] P. Cortes, J. Rodriguez, C. Silva, and A. Flores, "Delay compensation in model predictive current control of a three-phase inverter," *IEEE Trans. Ind. Electron.*, vol. 59, no. 2, pp. 1323–1325, Feb. 2012.
[21] D. Casadei, G. Serra, A. Stefani, A. Tani, and L. Zarri, "DTC drives for wide speed range applications using a robust flux-weakening algorithm," *IEEE Trans. Ind. Electron.*, vol. 54, no. 5, pp. 2451–2461, Oct. 2007.
[22] Y. Zhang, B. Xia, and H. Yang, "Performance evaluation of an improved model predictive control with field oriented control as a benchmark," *IET Elect. Power Appl.*, vol. 11, no. 5, pp. 677–687, 2017.
[23] S. A. Davari, D. A. Khaburi, F. Wang, and R. M. Kennel, "Using full order and reduced order observers for robust sensorless predictive torque control of induction motors," *IEEE Trans. Power Electron.*, vol. 27, no. 7, pp. 3424–3433, Jul. 2012.
[24] M. Siami, D. A. Khaburi, A. Abbaszadeh, and J. Rodríguez, "Robustness improvement of predictive current control using prediction error correction for permanent-magnet synchronous machines," *IEEE Trans. Ind. Electron.*, vol. 63, no. 6, pp. 3458–3466, Jun. 2016.

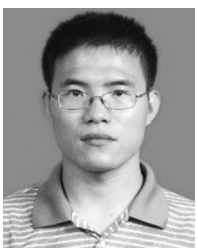

Yongchang Zhang (M'10–SM'18) received the B.S. degree in electrical engineering from Chongqing University, Chongqing, China, in 2004, and the Ph.D. degree in electrical engineering from Tsinghua University, Beijing, China, in 2009.

From August 2009 to August 2011, he was a Post-Doctoral Fellow with the University of Technology Sydney, Ultimo, Australia. He joined the North China University of Technology in August 2011 as an Associate Professor. He is currently a Full Professor and the Director with the Inverter Technologies Engineering Research Center of Beijing. He has authored and coauthored more than 100 technical papers in the area of motor drives, pulsewidth modulation, and ac/dc converters. His current research interests include model predictive control for power converters and motor drives.

Boyue Zhang was born in 1993. He received the B.S. degree in electrical engineering and automation from Liaoning Technical University, Liaoning, China, in 2017. He is currently working toward the master's degree in electrical engineering with the North China University of Technology, Beijing, China.

His research interests include model predictive control of induction motor drives.

Haitao Yang (S'16) received the B.S. degree in electrical engineering from the Hefei University of Technology, Hefei, China, in 2009, and the M.S. degree in electrical engineering from the North China University of Technology, Beijing, China, in 2015. He is currently working toward the Ph.D. degree in mechanical engineering with the School of Mechanical and Mechatronic Engineering, University of Technology Sydney, Sydney, Australia.

His research interests include motor drives, position/speed sensorless control of ac motors, pulsewidth modulation converters, and electric vehicles.

Margarita Norambuena (S'12–M'14) received the B.S. and M. S. degrees in electric engineering from the Universidad Tecnica Federico Santa Maria (UTFSM), Valparaiso, Chile, in 2013, the Ph.D. degree (summa cum laude) in electronics engineering from the UTFSM, in 2017, and the Doktoringenieur (Dr-Ing.) degree (summa cum laude) from the Technische Universitat Berlin (TUB), Berlin, Germany, in 2018.

She received a scholarship from the Chilean National Research, Science and Technology Committee, in 2014, to pursue the Ph.D. degree studies in power electronics with the UTFSM and the TUB. She also received a scholarship from the German Academic Exchange Service, in 2015, to pursue the Ph.D. degree studies with the TUB. She was an Assistant Professor with Universidad Andres Bello, Santiago, Chile. She is currently an Assistant Professor with UTFSM. Her research interest include multilevel converters, model predictive control of power converters and drives, energy storage systems, renewable energy, and microgrid systems.

Jose Rodriguez (M'81–SM'94–F'10) received the Engineering degree in electrical engineering from the Universidad Tecnica Federico Santa Maria, Valparaiso, Chile, in 1977, and the Dr.-Ing. degree in electrical engineering from the University of Erlangen, Erlangen, Germany, in 1985.

He has been with the Department of Electronics Engineering, Universidad Tecnica Federico Santa Maria, since 1977, where he was a Full Professor and the President. Since 2015, he has been the President with the Universidad Andres Bello, Santiago, Chile. He has coauthored two books, several book chapters, and more than 400 journal and conference papers. His main research interests include multilevel inverters, new converter topologies, control of power converters, and adjustable-speed drives.

Dr. Rodriguez has received a number of Best Paper awards from journals of the IEEE. He is a Member of the Chilean Academy of Engineering. In 2014, he received the National Award of Applied Sciences and Technology from the Government of Chile. In 2015, he received the Eugene Mittelmann Award from the Industrial Electronics Society of the IEEE.